

MAGHEMITE@SILICA NANOPARTICLES FOR BIOLOGICAL APPLICATIONS

S. Momet, E. Grasset*, J. Portier and E. Duguet

Institut de Chimie de la Matière Condensée de Bordeaux ICMCB-CNRS, Université Bordeaux-I, 87 avenue du Dr Albert Schweitzer, F-33608 Pessac, France * *Current address: Laboratoire des Verres et Céramiques, Institut de Chimie de Rennes, Université Rennes-I, Campus de Beaulieu, F-35042 Rennes, France*

INTRODUCTION

There is a great deal of interest in investigating new synthetic routes, controlling the size and the morphology, and understanding the overall behavior of nanoparticles. Magnetic nanoparticles are being studied in particular for their current and future applications in biology and medicine, including magnetic cell separation, magnetic resonance imaging contrast enhancement, magnetic transport of anti-cancer drugs [1].

In this field and especially for *in vivo* applications, the main challenges currently consist in (i) reducing the nanoparticle size for going through the majority of biological membranes, (ii) ensuring their stability in pH conditions of biological fluids and (iii) tailoring their surface in order to functionalize and/or develop strong interactions with specific biological components (dye, drug or effector grafting).

The magnetic nanoparticles, which are the most frequently studied, belong to the ferrite family, especially magnetite (Fe_3O_4) and maghemite ($\gamma\text{-Fe}_2\text{O}_3$). Many studies focused on ferrofluids, which are colloidal aqueous solutions (sols) of monodomain magnetic particles. Ferrofluids necessitate a sufficient electrostatic repulsion between particles [2]. Nevertheless, the zero point of charge (ZPC) of these iron oxides is close to 7. Aqueous ferrofluid dispersions therefore flocculate in the pH range of 5 to 9 and are stable only under highly acidic or basic conditions. On the other hand, the ZPC of SiO_2 is about 2-3 and therefore silica nanoparticles are negatively charged at pH 7 and consequently their dispersions in biological media would be stable.

For this reason we investigated the route consisting of encapsulating preformed maghemite nanoparticles in the ferrofluid state into silica. We hoped to obtain core-shell nanoparticles, denoted $\gamma\text{-Fe}_2\text{O}_3@SiO_2$, which (i) would form a stable dispersion in the pH conditions of biological fluids, (ii) would have sufficiently powerful magnetic properties and (iii) would have an easy surface chemistry thanks to the well-known reactivity of silica towards coupling agents, such as the

numerous commercially available alkoxy silane derivatives.

The synthetic method was derived from the Stöber process of silica nanoparticles synthesis (based on the base-catalyzed polycondensation of tetraalkoxysilane) and developed in reverse microemulsion conditions [3]. This technique relies on the self-assembly nature of surfactants to push aqueous reactant into micelles. Due to the dynamic nature of micelles, aqueous components (including maghemite nanoparticles) can come together and react to form particles, which are constrained to the micelle size.

The goals of the present study are to (i) control the $\gamma\text{-Fe}_2\text{O}_3@SiO_2$ morphology thanks to the synthesis conditions, (ii) investigate their stability in water, their thermal behavior and their magnetic properties and (iii) use them, secondarily, as precursors for silica hollow nanospheres, obtained by a discriminatory dissolution of the magnetic cores.

METHODS

Materials: all the chemicals (from Aldrich) were of reagent grade and used without further purification.

Ferrofluid synthesis: cationic $\gamma\text{-Fe}_2\text{O}_3$ aqueous sols were prepared according to the Massart's method [2]. The Fe_3O_4 precipitate, obtained by alkalinizing FeCl_2 and FeCl_3 ($\text{Fe}^{2+}/\text{Fe}^{3+} = 1/2$) aqueous mixture, was oxidized successively with 2 M HNO_3 and 0.33 M FeNO_3 solutions until the $\text{Fe}^{2+}/\text{Fe}^{3+}$ ratio in the particles was lower than 0.05 and therefore until magnetite was converted to maghemite. After removing by centrifugation, the particles were peptized in 2 M HNO_3 solution under vigorous stirring in order to create positive surface charges. The acidic precipitate was isolated by decantation on a magnet, washed in acetone and dispersed in pure water at $\text{pH} \approx 2.5$ in order to obtain an iron concentration of 0.125 M.

$\gamma\text{-Fe}_2\text{O}_3@SiO_2$ synthesis: both types of surfactants were simultaneously used: an ionic one which is dioctyl sulfocinate, sodium salt (AOT) and a nonionic one, which is polyoxyethylene (4) lauryl

ether (Brij®30). W/O microemulsions were prepared by adding the aqueous ferrofluid (whose pH was first adjusted with KOH in the range of 2.5-4.5) into a stirred solution of Brij®30/AOT (weight ratio 1/2) in heptane. Then, tetraethoxysilane (TEOS) was added. TEOS is an organophilic molecule and therefore is more readily dissolved in heptane than in aqueous micelles. Nevertheless, the presence of the acidic ferrofluid catalyzes TEOS hydrolysis. We supposed that after 15 min, the main part of TEOS has been pre-hydrolyzed and consequently has migrated into the micelles. Lastly, ammonia solution (30 wt.%) was added to catalyze the polycondensation of the prehydrolyzed TEOS into silica. The weight ratio of ferrofluid/TEOS/ammonia used in all experiments was 2.2/5.3/3. After 20 h, nanoparticles were washed with ethanol and chloroform to remove heptane and surfactant. The powder was dried at 60°C under vacuum for thermal, magnetic and BET studies.

$\gamma\text{-Fe}_2\text{O}_3@SiO_2$ aqueous dispersion preparation: microemulsions were washed as previously described, but without the drying operation. Then, a 0.5 M KOH aqueous solution was added on the flocculate and mixed in a vortex agitator. The addition of 10 volumes of acetone allowed the mixture to flocculate. In order to obtain the alkaline dispersion, the flocculate was peptized, after centrifugation, by addition of water.

SiO_2 hollow spheres synthesis: the flocculates of $\gamma\text{-Fe}_2\text{O}_3@SiO_2$ were leached by 10 M HCl solution in order to dissolve the maghemite cores. The flocculates were washed with water and centrifuged to remove the $FeCl_3$, until the yellow color vanished. The so-neutralized flocculate was then peptized the alkaline way as for the $\gamma\text{-Fe}_2\text{O}_3@SiO_2$ flocculates.

Characterization techniques: transmission electron microscopy (TEM) experiments were performed with a JEOL 2000 FX operating at an accelerating voltage of 200 kV. Samples for TEM were prepared on copper grids coated with a carbon support film (Pelco International) by evaporating a drop of particles dispersion. Specific surface areas were measured by nitrogen adsorption (BET method) using a Micromeritics ASAP 2010. The zeta potential titrations were obtained using a Zetasizer instrument of Malvern Corporation. Magnetic measurements were achieved using a susceptometer MANICS and SQUID 5MPMS.

RESULTS AND DISCUSSION

Shape and size of nanoparticles: the morphology of the pristine $\gamma\text{-Fe}_2\text{O}_3$ nanoparticles was observed by transmission electron microscopy (TEM). It was observed that maghemite particles are spherical with a diameter ranging between 5-10 nm (Fig. 1). BET measurements gave a specific surface area of 130 m²/g. The X-ray diffraction pattern at room temperature (not shown here) is consistent with the spinel structure.

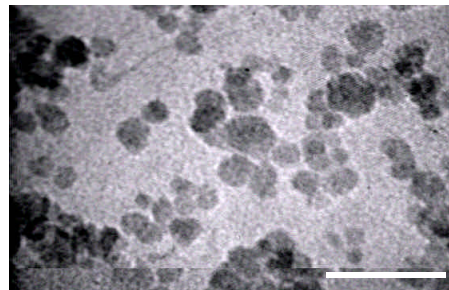


Fig. 1: TEM micrograph of $\gamma\text{-Fe}_2\text{O}_3$ nanoparticles extracted from the ferrofluid (scale bar: 50 nm)

Fig. 2 displays TEM pictures of $\gamma\text{-Fe}_2\text{O}_3@SiO_2$ nanoparticles vs. the initial pH of maghemite ferrofluids. It can be noticed that, in the studied pH range, the lower the pH value, the best dispersed the maghemite nanoparticles and therefore the lower the number of magnetic cores per silica shell. So, when the value of pH is close to the flocculation pH of 5, the aggregates of maghemite form chains and the morphology of core-shell particles is less well-defined (Fig. 2e).

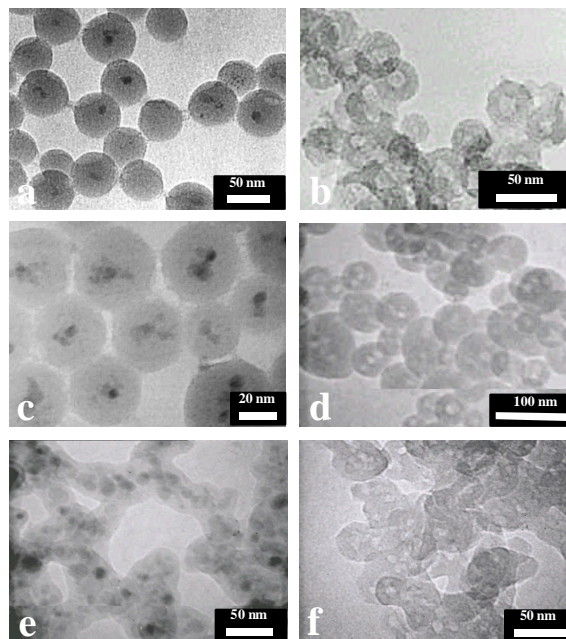


Fig. 2: TEM micrographs of $\gamma\text{-Fe}_2\text{O}_3@SiO_2$ nanoparticles vs. the initial pH of maghemite ferrofluids (a : pH 2.5; c : pH 3.5; e : pH 4.5) and their corresponding silica hollow spheres (b, d and f, respectively).

For the particular condition of the ternary system (water/surfactant/heptane) used in this study, it appears that pH is the main parameter that governs the morphology of the $\gamma\text{-Fe}_2\text{O}_3\text{@SiO}_2$ nanoparticles and the number of maghemite cores per silica shell.

BET measurements gave a specific surface area of $440\text{ m}^2/\text{g}$ for core-shell particles displayed on Fig. 2a, which suggests that the silica shell is highly porous. This feature might allow the dissolution of the maghemite core.

The electron microscopy pictures of the silica hollow spheres confirm that the maghemite cores have disappeared (Fig. 2b, 2d and 2f). Their diameter is close to that of their parent core-shell particles (in the range of 50 nm), demonstrating the discriminatory mechanism of the dissolution process. The size and number of holes seem to depend directly on the size and number of maghemite cores. Their specific surface area is higher than that of their parent core-shell particles ($480\text{ m}^2/\text{g}$ versus $440\text{ m}^2/\text{g}$).

Properties of $\gamma\text{-Fe}_2\text{O}_3\text{@SiO}_2$ ferrofluids: Zeta potential titrations as a function of pH (obtained by adding 0.01 M HNO_3 or KOH solutions) allowed to verify the value of 7 for maghemite ZPC and the flocculation of the nanoparticles in the pH range from 5 to 9 (Fig. 3). The presence of the silica shell decreased this value close to the silica ZPC (*i.e.* 2.5) and $\gamma\text{-Fe}_2\text{O}_3\text{@SiO}_2$ dispersions are stable for a pH higher than 5. However, it is well known that silica will readily dissolve under highly basic conditions.

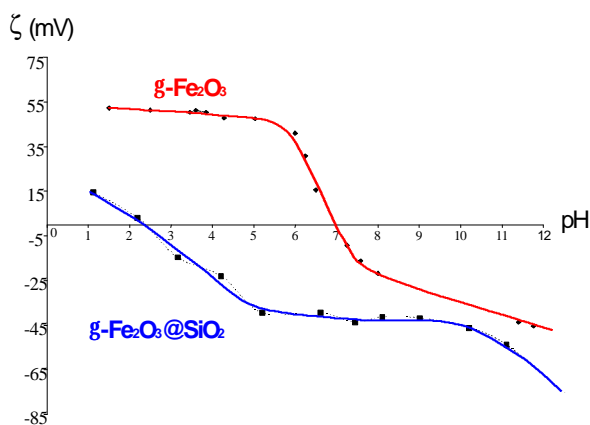


Fig. 3: Zeta potential titration as a function of pH of the $\gamma\text{-Fe}_2\text{O}_3$ dispersion and $\gamma\text{-Fe}_2\text{O}_3\text{@SiO}_2$ dispersion (synthesized from the ferrofluid in Fig. 2a with initial pH of 2.5).

Thermal behavior: As already observed for nanoparticles embedded in silica monoliths [4], the $\gamma\text{-Fe}_2\text{O}_3$ nanoparticles, obtained by drying the aqueous sol, transform into hematite ($\alpha\text{-Fe}_2\text{O}_3$) at around 673 K, whereas the $\gamma\text{-Fe}_2\text{O}_3$ cores in the $\gamma\text{-Fe}_2\text{O}_3\text{@SiO}_2$

materials remain unaltered until 1273 K (100° step and aging at this temperature for 1 h ; X-ray diffraction patterns not shown here). $\alpha\text{-Fe}_2\text{O}_3$ appears only at 1473 K, which is a further proof of the maghemite encapsulation by silica.

Magnetic properties: Typical zero field cooled (ZFC) and field cooled magnetization (FC) are plotted vs. temperature in Fig. 4. Such a behavior is characteristic of superparamagnetism and is due to the progressive blocking of the magnetization of smaller and smaller particles when temperature is decreasing. The temperature at which the ZFC and the FC curves get separated indicates the onset of blocking for the largest $\gamma\text{-Fe}_2\text{O}_3$ particles, while the maximum temperature in the ZFC curve can be related to the blocking temperature with the average volume.

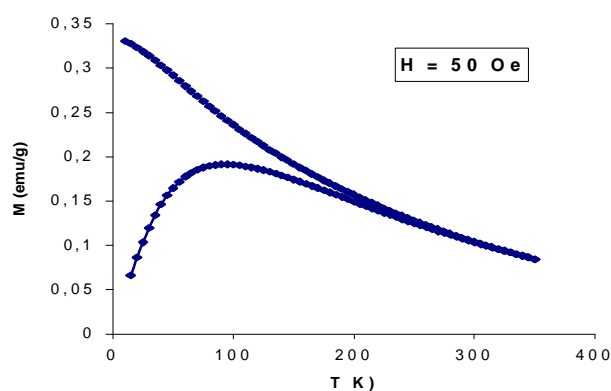


Fig. 4: ZFC and FC curves vs. temperature of $\gamma\text{-Fe}_2\text{O}_3\text{@SiO}_2$ (synthesized from the ferrofluid in Fig. 2a with initial pH of 2.5).

The field dependent hysteresis loops were measured at temperatures both below and above the blocking temperature. Fig. 5 shows the hysteresis curves at 15 K and 150 K. The magnetization vs. data at 15 K displays some hysteresis and confirms that the $\gamma\text{-Fe}_2\text{O}_3$ nanoparticles are ferrimagnetic below the blocking temperature. The absence of coercive hysteresis at 150 K (above the blocking temperature) is characteristic of superparamagnetic particles. Fig. 6 shows the hysteresis loops at 15 K of $\gamma\text{-Fe}_2\text{O}_3$ -silica annealed at different temperature. The observed magnetic behavior confirms that $\gamma\text{-Fe}_2\text{O}_3$ nanoparticles embedded in a silica shell remain stable until 1273 K and are in agreement with X-ray diffraction data. When the field is reduced, the magnetization M_r , known as the remnant magnetization at $H = 0$, remained identical until 1273 K. At 1473 K, the very weak signal observed was attributed to the transformation of the ferrimagnetic $\gamma\text{-Fe}_2\text{O}_3$ to the canted antiferromagnetic $\alpha\text{-Fe}_2\text{O}_3$.

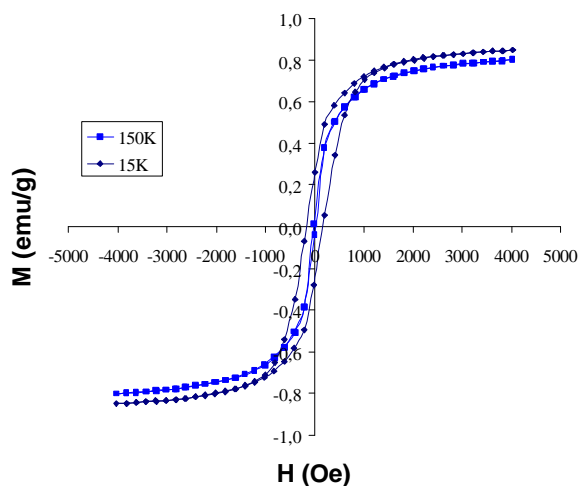


Fig. 5: Hysteresis loops at 15 K and 150 K of $\gamma\text{-Fe}_2\text{O}_3@SiO_2$ nanoparticles.

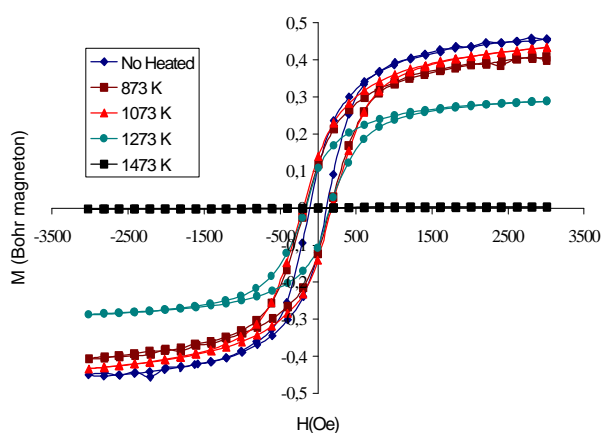


Fig. 6: Hysteresis loops at 15 K of $\gamma\text{-Fe}_2\text{O}_3@SiO_2$ annealed at different temperatures.

CONCLUSION AND PERSPECTIVES

We have presented a reverse microemulsion technique, demonstrating the feasibility of synthesizing $\gamma\text{-Fe}_2\text{O}_3@SiO_2$ nanoparticles with a size of a few tens of nanometers. The initial pH of the ferrofluid seems to play an important role in the morphology of the materials and allows to control the number of magnetic cores per silica shell. These $\gamma\text{-Fe}_2\text{O}_3@SiO_2$ nanoparticles were dispersed in aqueous phase and the ZPC of the new ferrofluid was measured at pH 2.5. Maghemite nanoparticles with a silica shell may therefore be readily dispersed in water in the pH range from 5 to 11, making them stable in biological fluids. Magnetic experiments have shown that maghemite nanoparticles preserve their superparamagnetic properties, despite being embedded in silica shells.

Currently, further experiments are in progress to (i) investigate new water/AOT/Brij30[®]/heptane ratios in order to vary the micelle size and therefore the thickness of the silica shell and (ii) functionalize the

surface of the silica shells with various alkoxy silane derivatives and then with molecules of biological and medical interest.

Concerning the silica hollow nanospheres, our study has demonstrated the possibility to obtain them through a discriminatory dissolution technique with a good correlation between the magnetic core number and the hole number. We are focusing our efforts on their potential applications as (non magnetic) drug carriers or as nanoreactors for (magnetic) materials whose synthesis in nanoparticle form is not known. For such applications, the core would be loaded with the precursor and the silica shell could act as a rigid template. It would be stable even during the high temperature treatment of solid state chemistry, and finally would be dissolved under basic conditions to release the new materials.

REFERENCES: ¹Scientific and Clinical Applications of Magnetic Microspheres (1997), (eds. U. Häfeli, W. Schütt, J. Teller and M. Zborowski) Plenum Press, New York. ²R. Massart (1982) *IEEE Trans Magn* **17**:1247. ³S. Mornet, F. Grasset, E. Duguet and J. Portier (2000) *Proceedings of the Eighth International Conference on Ferrites, Kyoto and Tokyo*, ed. by the Japan Society of Powder and Powder Metallurgy, pp 766-8. ⁴E. Tronc, C. Chanéac and J.P. Jolivet (1998) *J Solid State Chem* **139**:93.

ACKNOWLEDGMENTS: The Groupe d'Intérêt Scientifique "Vectorisation *in vivo*" is gratefully acknowledged for its financial and scientific support. The authors are deeply grateful to L. Albingre for BET measurements, E. Lebraud for the in-temperature X-ray diffraction measurements and E. Sellier for carrying out the electron microscopy observations.